INTERNATIONAL JOURNAL OF APPLIED AND EXPERIMENTAL BIOLOGY
(ISSN PRINT: 2790-6523; ISSN ONLINE: 2790-6531)
2025, Vol. 4, NO. 1, 27-39
DOI: https://doi.org/10.56612/ijaaeb.v1i1.107
ARK: https://n2t.net/ark:/71142/IJAaEB.v1i1.107
https://eminentscientists.com/

Biofabricated silver nanoparticles from *Calotropis procera*: A potential antimicrobial solution against pathogenic bacteria

Muhammad Maisam[1], Madeeha Shahzad Lodhi[1], Sumaira Sharif[1], Ruqiya Anees[1], Rana Ismail Anwar[1], Muhammad Inam[2], Ihtisham Bukhari[3]

[1]Institute of Molecular Biology and Biotechnology (IMBB), The University of Lahore. 1 km Defence Road, Lahore, 58810, Pakistan.
[2]College of Pharmaceutical Science, Guangzhou Medical University, Guangzhou, China.
[3]Principal Investigator/Associate Professor (Overseas High Talent Researcher) Marshall B.J Medical research Centre, Fifth, Affiliated Hospital Zhengzhou University, Zhengzhou, China

Abstract

Calotropis procera has the potential as a traditional medicinal plant that offers a diverse array of healing treatments. It was used in conventional medicine to remedy several ailments, including diarrhea and snakebites. This study examines the antibacterial properties of silver nanoparticles derived from the floral and latex components of *C. procera*. The nanoparticles were tested for their effectiveness against Gram-negative and Gram-positive bacterial strains. For characterization, the synthesized nanoparticles underwent thorough analysis using UV spectroscopy, fourier-transform infrared spectroscopy (FTIR), X-ray diffraction (XRD), and scanning electron microscopy (SEM). After the reduction process, the FTIR analysis revealed that some functional biomolecules found in plants form a coating on the nanoparticles, serving as organic agents that stabilize the nanoparticles. The size of nanoparticles analyzed with SEM falls in the 30 to 130 nm range. Furthermore, the synthesized silver nanoparticles were tested as antimicrobial agents against *Escherichia coli*, *Bacillus subtilis*, *Staphylococcus aureus*, and *Pseudomonas aeruginosa*, well-known microorganisms that can produce ulceration phases and severe health consequences. After a comprehensive examination, it was found that the silver nanoparticles have significant antibacterial effectiveness, particularly against *S. aureus*, a primary bacterium responsible for causing different ailments. The remarkable antibacterial efficacy of the silver nanoparticles synthesized in an environment-friendly manner underscores its potential applications in combating the evolution of antibiotic-resistant strains.

ARTICLE TYPE
Research Paper (RP)

SECTION
Microbiology (MB)

HANDLING EDITOR
Ashraf, M.A.B. (HB)

ARTICLE HISTORY
Received: 02 May, 2024
Accepted: 22 Oct, 2024
Online: 22 Oct, 2024
Published: 06 Jan, 2025

KEYWORDS
Bacillus subtilis;
Drug-resistant bacteria;
Escherichia coli;
Green Synthesis;
Pseudomonas aeruginosa;
Staphylococcus aureus

Introduction

The increasing challenge of drug-resistant bacteria has become a significant threat to human health. Thus, in the scenario of increasing resistance to antibacterial agents, taking precautions to protect

***CONTACT** Madeeha Shahzad Lodhi, madeeha.shahzad@imbb.uol.edu.pk, ☎ Ph: +92-42-111865865 Institute of Molecular Biology and Biotechnology (IMBB), The University of Lahore. KM Defence Road, Lahore (58810), Pakistan

CITATION (APA): Maisam, M., Lodhi, M.S., Sharif, S., Anees, R., Anwar, R.I., Inam, M., Bukhari, I. (2025). Biofabricated silver nanoparticles from *Calotropis procera*: A potential antimicrobial solution against pathogenic bacteria. *International Journal of Applied and Experimental Biology* Vol. 4(1), 27-39.

human well-being is becoming indispensible. Thus, the continuous search for new therapeutic agents is a plausible approach. Many compounds with a strong antimicrobial activity have been widely found in medicinal plants (Antwi et al., 2017).

Escherichia coli, Bacillus subtilis, Staphylococcus aureus, Pseudomonas aeruginosa, and Shigella species are infectious bacteria that can cause various infections. These include bloody diarrhea caused by *E. coli* and *Shigella* spp., and acteremia and endocarditis caused by *S. aureus*. These bacteria also cause skin and tissue infections and infections in the blood and lungs (Linz et al., 2023). Abscesses are a disease caused by *Streptococcus aureus* in which a painful collection of pus is formed. In some cases, the pus develops inside the skin; in others, it develops inside the organs or the spaces between them (Conan et al., 2021).

Calotropis procera is an evergreen xerophytic medicinal plant that occurs widely in a dry and semi-arid habitat. This plant is used habitually in medicine in the Middle East, South Asia, and North Africa (Farahat et al., 2015). Its leaves are used for medicinal purposes, mainly as the antidote for snack bites, sinus fistula, rheumatism, mumps, burn injuries, jaundice, and body pain treatments (Ferdosi et al., 2021). The plant also serves as another medicinal substance, such as antipyretic, antidiarrheal, antibacterial, anti-asthmatic, etc. *Calotropis procera* is a herbal remedy for arthritis illness. This plant is rich in latex and possesses strong anti-inflammatory, and weak antipyretic and analgesic action in various animal models. Some parts of this plant can be harmful to lives. The latex of *C. procera,* when in contact with eye causes painful corneal damage and instant dimness in the vision (Souza et al., 2022).

The leaves of *C. procera* also contain several active chemicals, including three glycosides named calotropin, uscharin, and calotoxin. Flowers and latex contain several phytochemicals, e.g., terpene, saponins, cardiac glycosides, and flavonoids are present in flowers, while tannins and resins are additional components reported in the latex (Rabelo et al., 2023). Latex is mainly used for ringworms, dog-bitten wounds, and skin diseases (Falana et al., 2020; Abbas et al., 2022).

Nanotechnology is an emerging field of science with many applications in the health industry. The use of nanotechnology can enhance the efficacy of medicinal compounds (Lodhi et al., 2021). Silver salt is well known for its antimicrobial activity, and this activity can be enhanced in the bioreduction of this silver and nucleation using medicinal compounds as reducing equivalents. These medicinal compounds fabricate the nanoparticles as stabilizing agents during the ripening phase (Singh et al., 2018).

This study was carried out to ascertain whether or not the *Calotropis procera* phytocompound fabricated silver nanoparticles have antimicrobial activity against *Pseudomonas aeruginosa, Streptococcus aureus, Escherichia coli, and Bacillus subtilis*. Thus, this study aimed to evaluate the antimicrobial and antioxidant properties of the green synthesized silver nanoparticles made from the plant extract of *C. procera* by using two parts of this medicinal plant, flower and latex.

Materials and Method

Preparation of plant extract

Calotropis procera flowers and latex were collected, carefully cleaned in deionized water and submerged for half an hour. The plant samples were then crushed to produce each sample of 25 g. The plant material was added to 100 mL of deionized water and heated in a water bath to 80–90 °C. When a color change was noticed, Whatman filtering was applied to the plant extract.

Green synthesis of silver nanoparticles

A solution of 10 mM $AgNO_3$ was prepared by taking 0.17 g of $AgNO_3$ and dissolving it in 100 mL of deionized water. This solution was boiled for 30 min and then an aliquot of 10 mL of the plant extract was added to it. The solution was heated at 80 °C with continuous stirring until a change in color to reddish brown was observed. The color shift indicated the green synthesis of Ag-NPs. The synthesized Ag-NPs were centrifuged at 9447 x *g* for 20 min, and the collected particles were rinsed and dried with acetone.

Characterization of nanoparticles

The synthesized phytofabricated silver nanoparticles were fully characterized by FTIR (Fourier transform infrared spectroscopy), UV-Vis (Ultra-violet visible spectrophotometry), DLS (Dynamic light scattering analysis), XRD (X-ray diffraction analysis), SEM (Scanning electron microscope) and EDX (Energy dispersive X-ray) to assess the morphology, size, and nature of nanoparticles. The plant extract was also characterized by FTIR and DLS (Dawadi et al., 2021).

Isolation of bacteria from soil

Two separate locations were used for collecting soil samples. A sanitized equipment was used to

isolate bacteria using the spread plate method. After making dilutions (up to 10^{-4} were serially diluted), and the diluted samples were spread out onto nutrient agar plates using the spread plate technique and followed by a 24-hour incubation period at 37 °C. The use of colony morphology, microscopic features, and biochemical assays made the identification of bacteria.

Biochemical testing

Different biochemical tests were performed to identify bacteria from a mixed culture (**Table 1**).

Table 1: Biochemical testing

Bacteria	Biochemical tests
Pseudomonas aeruginosa	Indole, methyl red, catalase, hemolysis test and urease test
Bacillus subtilis	Catalase test, indole test, methyl red test and citrate test
Escherichia coli	Indole test, citrate test, urease test and nitrate reduction test
Staphylococcus aureus	Catalase test, citrate test, hemolysis test and indole test

Well diffusion assay

The well diffusion assay (Fijan et al., 2022) was used to check the antimicrobial activity of four different bacterial species: *E. coli, S. aureus, P. aeruginosa,* and *B. subtilis*. For every bacterial strain, three Petri plates with four evenly spaced wells on solidified agar were made. The wells were designated as follows: well 1 held 25 µL, well 2 50 µL, well 3 75 µL, and well 4 held 100 µL. The zones of inhibition were then measured and evaluated after the agar plates were incubated for 24 h at 37 °C.

Results

Characterization of nanoparticles

FTIR

The FTIR results of silver salt, plant extract, and silver nanoparticles were analyzed with the frequency range of 4000-400 cm^{-1} (**Figure 1**). The silver salt FTIR analysis showed peaks assigned to different functional groups: C-H bending of aromatic compound, S=O stretching of sulfone group, O-H stretching of alcohol class, and C=C bending of alkene class. **Figure 1B** shows the extract FTIR spectra, which revealed the presence of functional groups such as amine group N-H bending, carboxylic acid group O-H bending, and aliphatic ether group C-O stretching. **Figure 1C** demonstrates the O-H stretching-related peaks in FTIR spectra of phytofabricated silver nanoparticles; the spinal structure of silver nanoparticles shows that the peaks lie in both the fingerprint region and group region for silver nanoparticles. Further, it confirms that the biomolecules in *Calotropis procera* are responsible for reducing and capping silver nanoparticles.

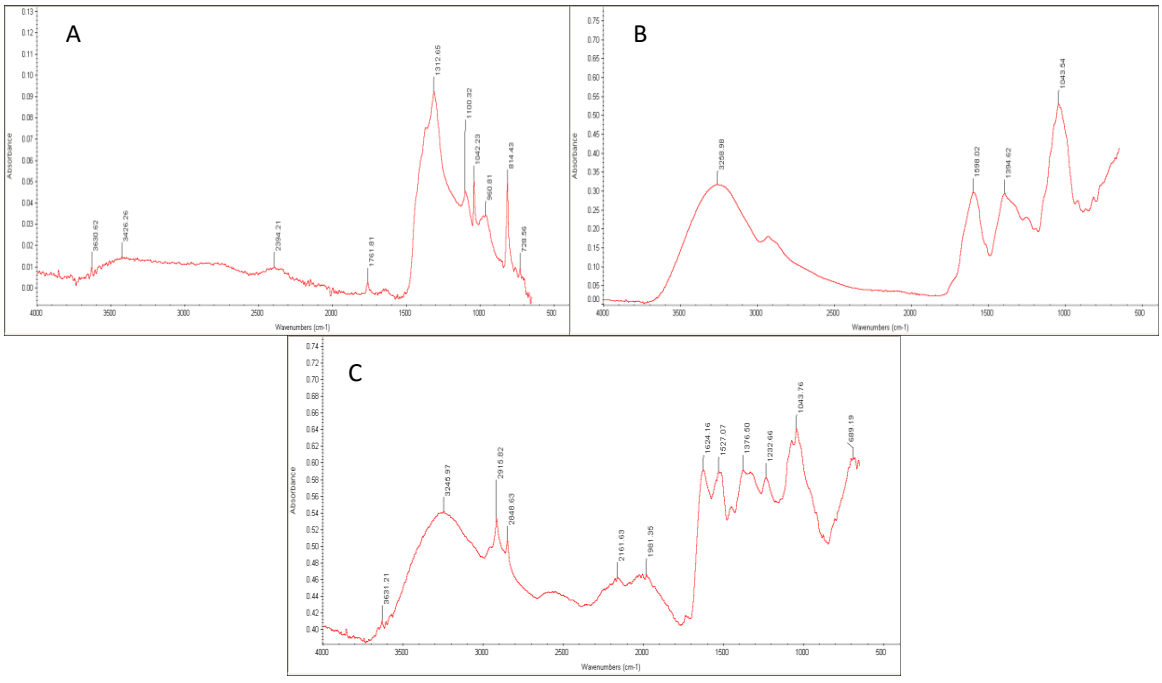

Figure 1: FTIR analysis of (A) silver salt, (B) plant extract, and (C) silver nanoparticles

UV-Vis spectrophotometry

The UV results were run for silver nanoparticles in the 200-800 nm range. The characteristic peak for silver nanoparticles was observed between 395-425 nm. Depending on the size and shape of the nanoparticles, the surface plasmon band was observed in both visible and infrared regions. Silver nanoparticle results showed the surface plasmon resonance in the visible region (**Figure 2**).

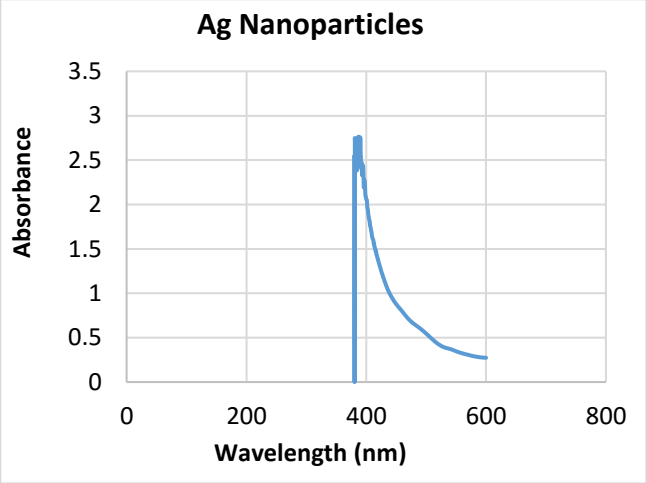

Figure 2: UV-Vis spectrum of phytofabricated silver nanoparticles

DLS analysis of nanoparticles

Figure 3 shows the size range of synthesized phytofabricated silver nanoparticles. Two peaks were observed in DLS analysis; peak 1 shows that the average size of silver nanoparticles is 149.89 nm with an area of 98.94%; peak 2 shows that almost 1% of particles fall in the size range of 5-10 nm with an average size of 8.3 nm. The hydrodynamic diameter is 121.36 nm, index 23.1%, polydispersity, and 4.0 $\mu m^2/s$ dilution coefficient.

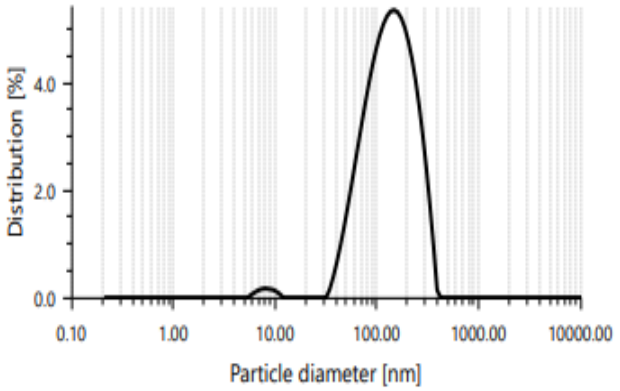

Figure 3: DLS analysis of nanoparticles

XRD analysis of nanoparticles

Figure 4 shows a diffractogram of silver nanoparticles. The diffraction peaks are observed at 2Θ= 14.6°, 15.1°, 20.7°, 28.2°, 31.8°, 38.1°, 38.5°, 40.4°, 43.1°, 43.2°, 44.5°, 45.5°, 47.0°, 48.5°, 50.3° with planes of (179), (179), (286), (282), (230), (249), (251), (257), (254), (253), (254), (263), (351), (259), and (237). At 31.8°, a strong peak with (230) plane was observed. These planes confirmed that the Ag nanoparticles have a face-centered cubic (FCC) structure corresponding to the JCPD file no. 31-1238 (Ali et al., 2023).

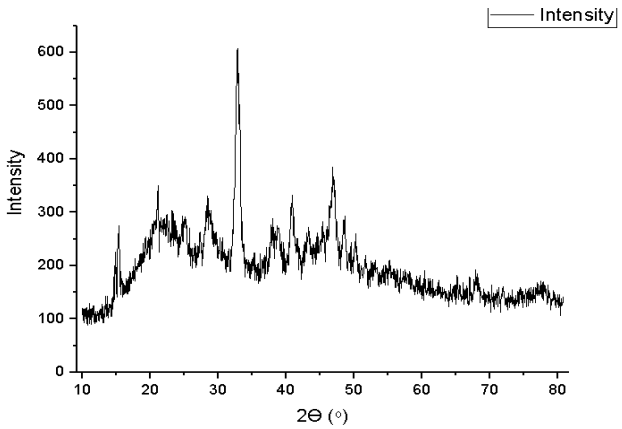

Figure 4: Diffractogram of Ag nanoparticles

SEM analysis

The SEM was performed to determine the size and shape of the synthesized nanoparticles. The Ag nanoparticles were found to be spherical in shape and had a size range of 30-110 nm with an average size of 50 nm. Some portions of the figure demonstrate that nanoparticles aggregated due to the presence of secondary metabolites in the plant extracts (**Figure 5**).

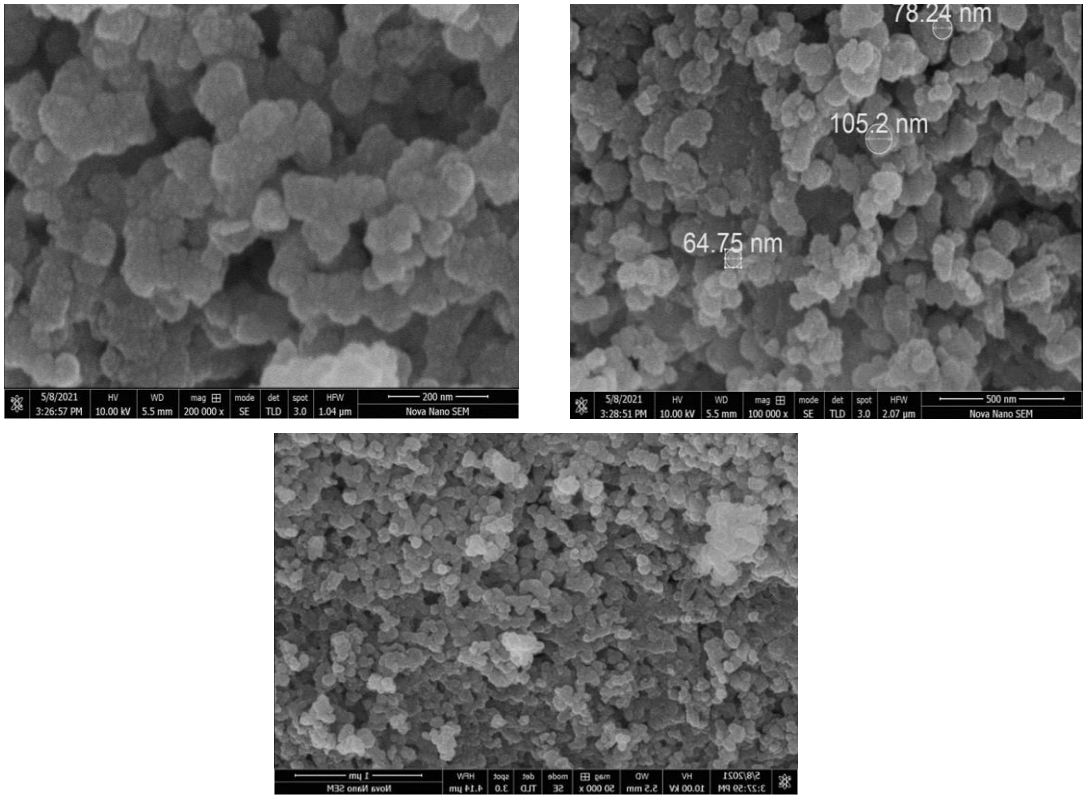

Figure 5: SEM analysis of Ag nanoparticles

EDX analysis

The EDX peaks show the presence of Ag, C, and O. Ag peak is shown at 0.0024 keV, and C and O at 0.08 keV (**Table 2**; **Figure 6**)

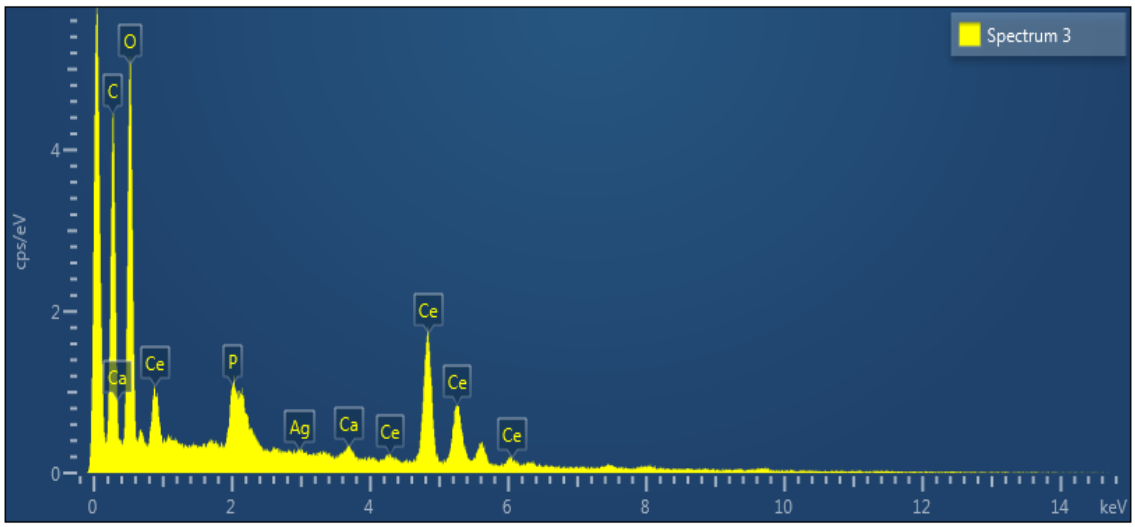

Figure 6: EDX analysis of Ag nanoparticles

Table 2: Elements present with Ag nanoparticles with their respective weights

Element	Line type	Apparent concentration	K ratio	Wt %
C	K series	8.89	0.08891	28.41
O	K series	25.25	0.08498	30.71
P	K series	1.44	0.00805	1.62
Ca	K series	0.48	0.00427	0.66
Ag	L series	0.24	0.0024	0.45
Ce	L series	20.57	1.1914	38.15
Total				100

Antimicrobial Activity

a. Pseudomonas aeruginosa

a.1. Biochemical identifications

Different experiments were performed to identify *P. aeruginosa* (**Figure 7**). The results show the positive confirmation of the strain isolated (**Table 3**).

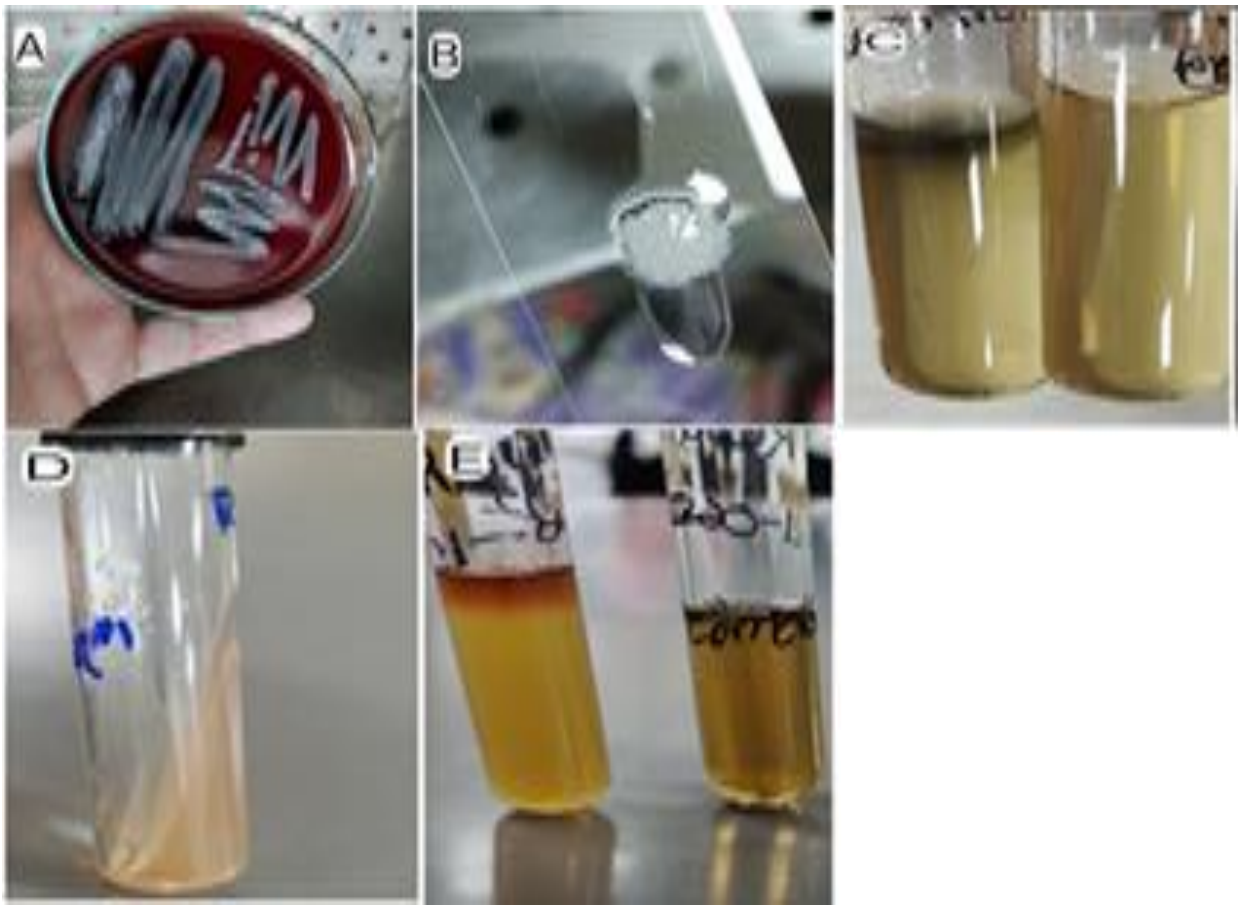

Figure 7: Biochemical tests of *P. aeruginosa,* (A) hemolysis test, (B) catalase test, (C) indole test, (D) urease test, and (E) methyl red test

Table 3: Biochemical identifications of *Pseudomonas aeruginosa*

Biochemical test	Results
Indole test	Negative
Methyl red test	Negative
Catalase test	Positive
Hemolysis	β-hemolysis
Urease test	Negative

a.2. Antimicrobial activity of synthesized phytofabricated silver nanoparticles against Pseudomonas aeruginosa

The well diffusion assay shows different inhibition zones at different concentrations (**Figure 8A** and **Figure 8B**). An inhibition zone of 10.5 mm was observed at 100 µL concentration, 13.5 at 125 µL, 15 mm at 150 µL, 18.5 mm at 200 µL, 19 mm at 250 µL and 21.5 mm at 500 µL. **Figure 8C** shows the comparative antimicrobial activity of the synthesized phytofabricated silver nanoparticles against *P. aeruginosa.*

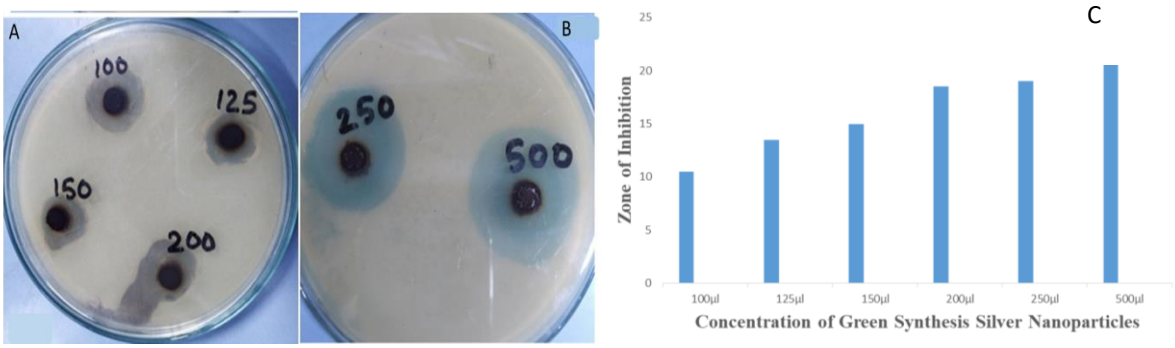

Figure 8: Antibacterial activity of phytofabricated Ag-NPs against *P. aeruginosa*. Figures 8A and 8B show inhibition zones at different concentrations of silver nanoparticles, and Figure 8C shows the comparative antimicrobial activity of silver nanoparticles against *P. aeruginosa*.

Bacillus subtilis

b.1. Biochemical identifications

Four biochemical tests were performed to identify *Bacillus subtilis*, namely the catalase, indole, methyl red, and citrate tests. **Figure 9** confirms the isolated strain of *Bacillus subtilis* (**Table 4**).

Table 4: Biochemical identifications of *Bacillus subtilis*

Biochemical test	Results
Catalase test	Positive
Indole test	Negative
Methyl red test	Negative
Citrate test	Positive

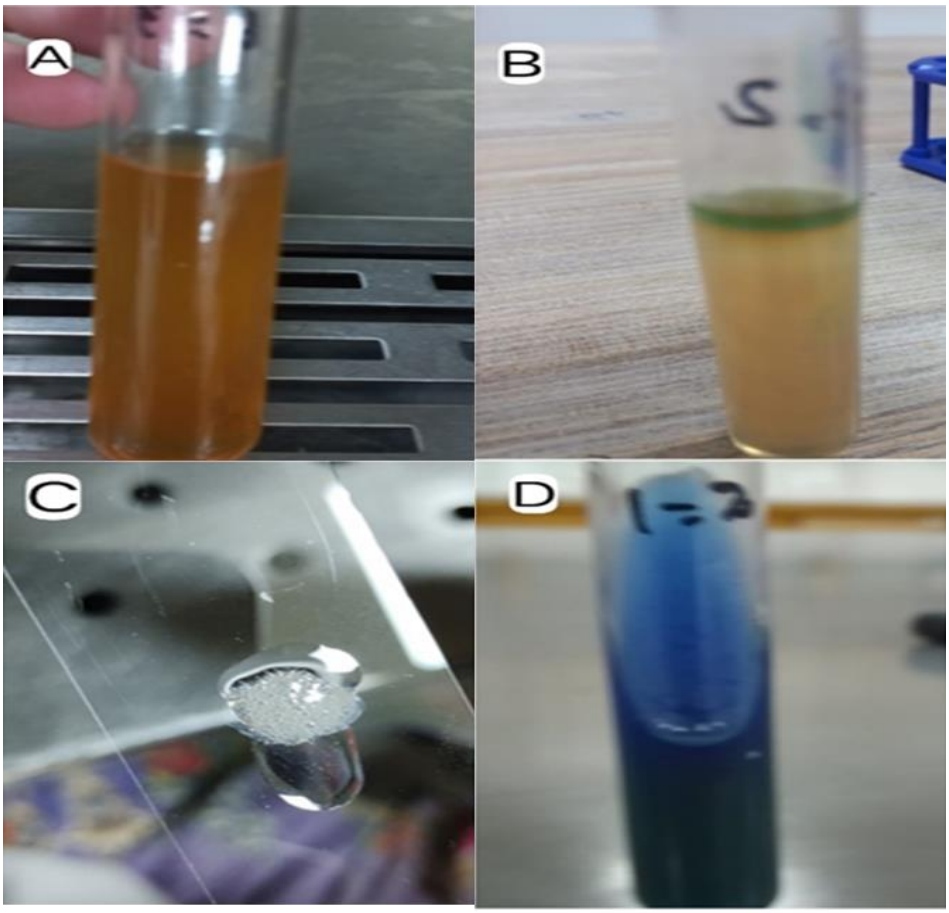

Figure 9: Biochemical testing of *B. subtilis,* (A) methyl red test, (B) indole test, (C) catalase test, and (D) citrate test

b.2. Antimicrobial activity of nanoparticles against Bacillus subtilis

The well diffusion assay shows different inhibition zones at different concentrations (**Figure 10A** and **Figure 10B**). An inhibition zone of 17 mm was observed at 100 µL concentration,18 mm at 125 µL, 22 mm at 150 µL, 24.5 mm at 200 µL, 25 mm at 250 µL, and 28 mm at 500 µL. **Figure 10 C** shows the comparative antimicrobial activity of the synthesized phytofabricated silver nanoparticles against *B.*

subtilis.

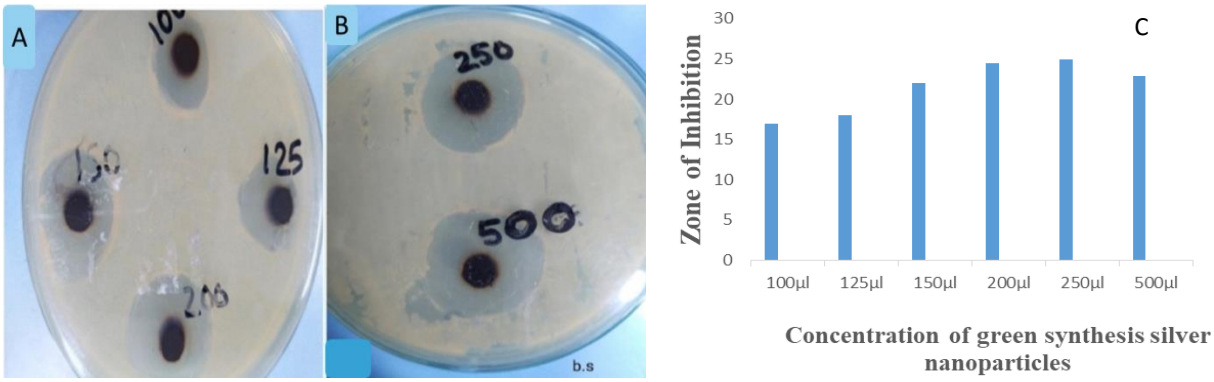

Figure 10: Antibacterial activity of phytofabricated Ag-NPs against *B. subtilis.* Figures A and B show inhibition zones at different concentrations of silver nanoparticles, and Figure C shows the comparative antimicrobial activity of silver nanoparticles against *B. subtilis.*

Staphylococcus aureus

c.1. Biochemical identifications

Different biochemical tests (hemolysis test, citrate test, catalase test, and indole test) were performed to confirm the isolated strain, and the results showed a positive confirmation of *S. aureus (***Figure 11**, **Table 5**).

Table 5: Biochemical test results of *S. aureus*

Biochemical test	Results
Catalase test	Positive
Citrate test	Positive
Hemolysis test	β-hemolysis
Indole test	Negative

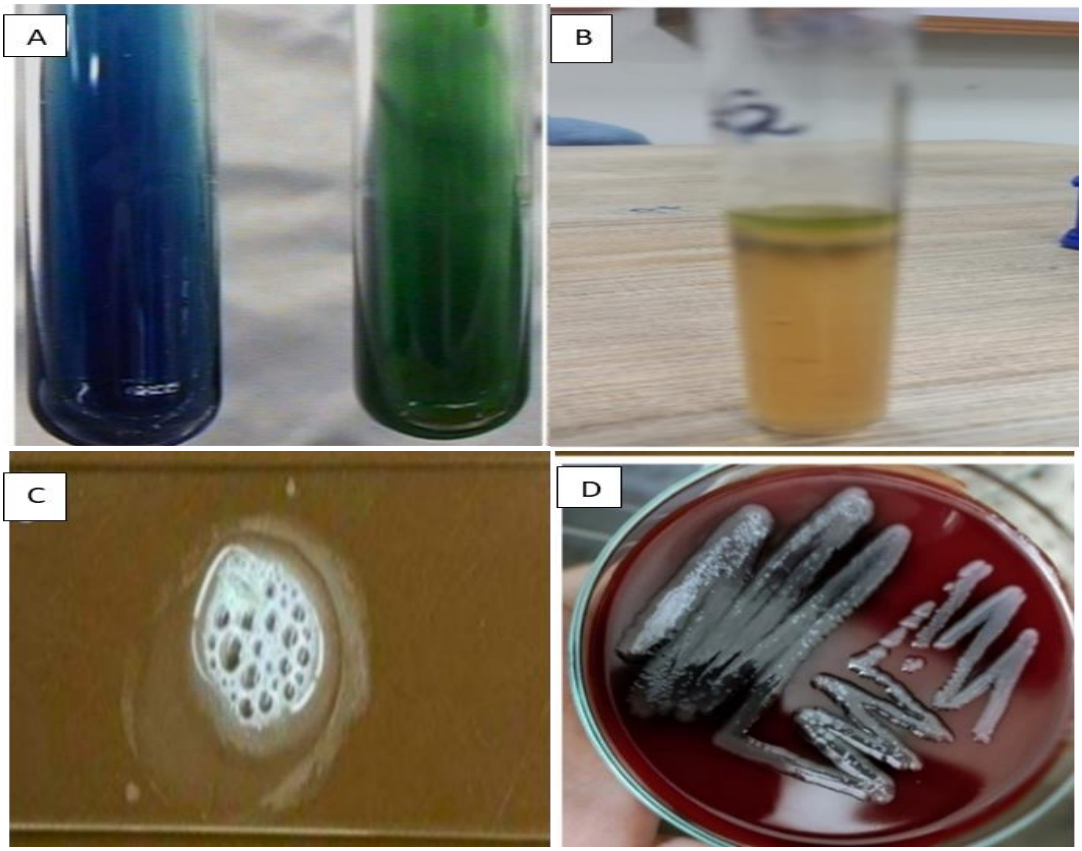

Figure 11: Biochemical tests of *S. aureus,* (A) citrate test, (B) indole test, (C) catalase test, and (D) hemolysis test

c.2.Antimicrobial activity of nanoparticles against Staphylococcus aureus

The well diffusion assay shows different inhibition zones at different concentrations (**Figure 12A** and **Figure 12B**). An inhibition zone of 19.5 mm was observed at 100 µL concentration, 21.55 mm at 125 µL, 22 mm at 150 µL, 22.5 mm at 200 µL, 23 mm at 250 µL, and 25 mm at 500 µL. **Figure 12C** shows the comparative antimicrobial activity of the synthesized phytofabricated silver nanoparticles against *S.*

aureus.

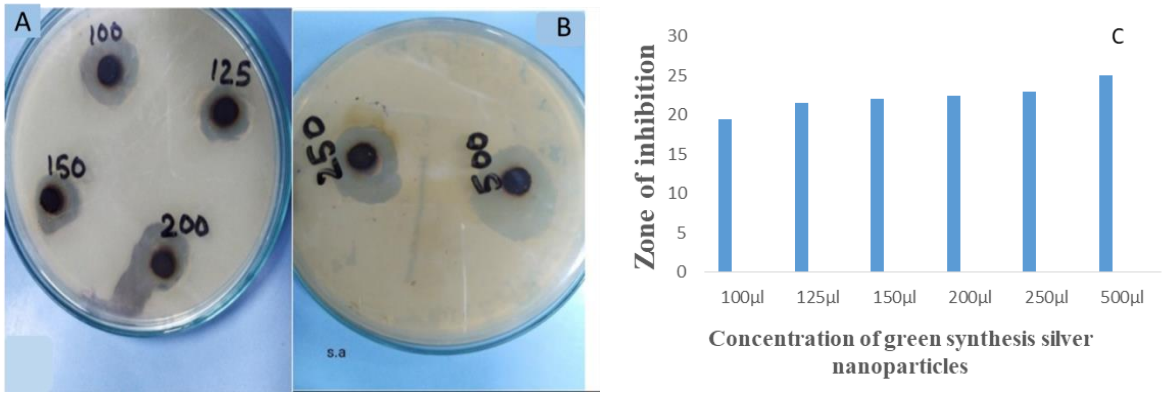

Figure 12: Antibacterial activity of phytofabricated Ag-NPs against *S. aureus.* Figures A and B show inhibition zones at different concentrations of silver nanoparticles, and Figure C shows the comparative antimicrobial activity of silver nanoparticles against *S. aureus.*

3.2.4 Escherichia coli

d.1. Biochemical identifications

Different biochemical tests (hemolysis test, citrate test, catalase test, and indole test) were performed to confirm the isolated strain, and the results showed a positive confirmation of *E. coli* (**Figure 13**, **Table 6**).

Table 6. Biochemical testing results of *E. coli*

Biochemical test	Results
Indole test	Positive
Citrate test	Negative
Urease test	Negative
Nitrate reduction	Positive

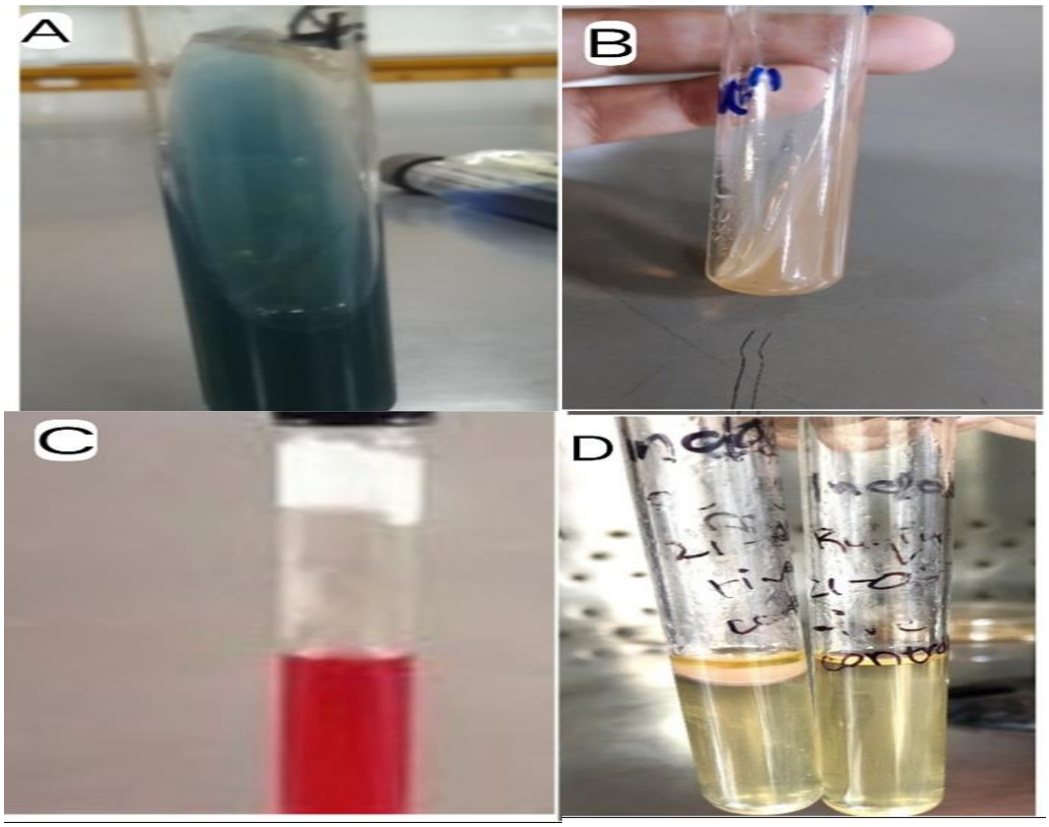

Figure 13: Biochemical testing of *E. coli,* (A) citrate test, (B) Urease test, (C) nitrate reduction test, and (D) indole test

d.2. Antimicrobial activity of nanoparticles against E. coli

The well diffusion assay shows different inhibition zones at different concentrations (**Figure 14A** and **Figure 14B**). An inhibition zone of 12.5 mm was observed at 100 µL concentration, 19.5 mm at 125 µL, 20 mm at 150 µL, 22.5 mm at 200 µL, 23 mm at 250 µL, and 25 mm at 500 µL. **Figure 14C** shows the comparative antimicrobial activity of the synthesized phytofabricated silver nanoparticles against *E. coli.*

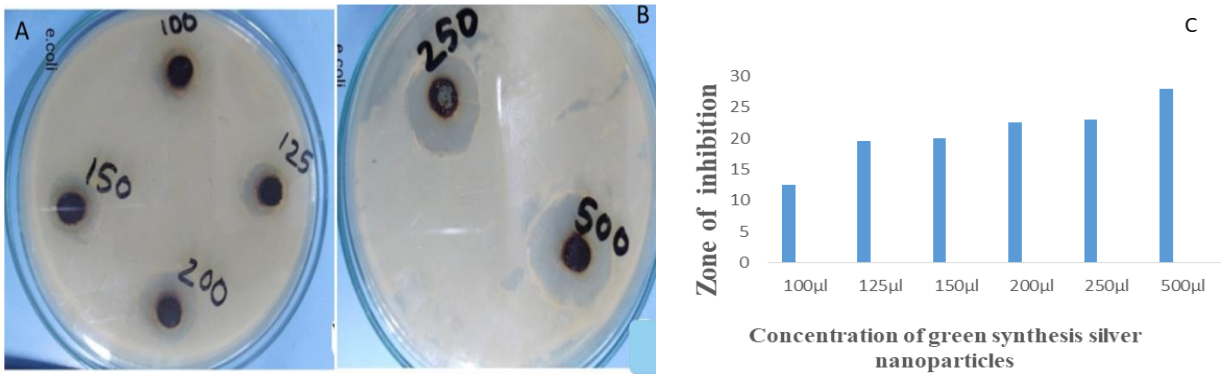

Figure 14: Antibacterial activity of phytofabricated Ag-NPs against *E. coli.* Figures A and B show inhibition zones at different concentrations of silver nanoparticles, and Figure C shows the comparative antimicrobial activity of silver nanoparticles against *E. coli.*

Discussion

Calotropis procera is a medicinal plant traditionally used to treat several diseases including diarrhea, somatic, sinus fistula, jaundice, and skin diseases (Murti et al., 2010). The effectiveness of this plant has already been tested at different research centers in different ways. Thus, in the current investigation, we assessed the antimicrobial activity of green synthesized silver nanoparticles using flower and latex of *C. procera* against common infection-causing microbes.

The flower and latex extracts of *C. procera* are believed to contain a myriad of chemical components, including triterpenes, alkaloids, cardiac glycosides, tannins, and flavonoids (Aliyu et al., 2015). These substances could be involved in the conversion of $AgNO_3$ salt to Ag nanoparticles (Ag-NP). Ag-NPs are produced when silver nitrate and plant extract interact. The resulting brown color recognizes Ag-NP-typical surface plasmon oscillations. The $AgNO_3$ solution under control (without extract) does not change color. The change in color of the silver solution during synthesis with a plant extract to reddish brown confirms the synthesis of silver nanoparticles (Ahmad et al., 2019). A brownish-black solution develops in the case of reduction with sodium borohydride (Mohamed et al., 2014).

The nanoparticle size, shape, and surface properties are among their distinct optical features, which were also examined in Ag-NPs using different characterizing techniques (Sancı and Volkan, 2009; Raghava et al., 2021). The functional groups that participated in synthesizing silver nanoparticles and stabilizing the complex were also well understood using FTIR spectroscopy (Deepa et al., 2013). The XRD analysis affirmed the FCC arrangement of planes for the synthesized metallic nanoparticles through prominent diffraction.

The DLS analysis showed the hydrodynamic size of synthesized silver nanoparticles as 149 nm. The SEM image of the silver nanoparticles displays the synthesized metallic Ag-NP exhibiting the array of morphology with a nonhomogeneous distribution with an average size of 50 nm (Asif et al., 2022). The size analysis through both techniques, DLS and SEM, showed a disparity, since the DLS analysis quantifies the hydrodynamic size in a liquid medium and its corresponding solvents, while SEM determines the size in a dry state and is considered to be more precise (Lodhi et al., 2021). However, solvents can influence the size distribution of nanoparticles.

For studying the antibacterial properties of green-produced Ag-NP, bacterial species were isolated and their identification was done using different biochemical tests.

Pseudomonas aeruginosa and *E. coli* are Gram-negative bacteria. *Pseudomonas aeruginosa* causes inflammation in the blood, lungs, or other body parts (Salomoni et al., 2017). *Escherichia coli* is found in the lower intestine of warm-blooded organisms. *Escherichia coli* can be the reason for bloody diarrhea, severe stomach cramps, food poisoning, and vomiting (Menichetti et al., 2023).

This study demonstrates that Ag-NP can exert substantial antibacterial effects against both *E. coli* and *P. aeruginosa*, as well as other bacteria that pose significant health risks. Higher concentrations of Ag-NPs showed a potent antimicrobial activity against *P. aeruginosa* and *E. coli*, forming larger inhibition zones. The results clearly depict that silver nanoparticles, mediated by *C. procera*, are a practical approach against both Gram-negative bacterial species. This suggests that these nanoparticles could be used to treat Gram-negative bacterial infections, underscoring their potential role in antibacterial therapy.

The antimicrobial efficacy of the synthesized phytofabricated silver nanoparticles was also analyzed against two harmful Gram-positive bacteria, specifically *B. subtilis* and *S. aureus*. It is widely reported that the excessive and unselective use of antibiotics exerts resistance in these bacterial species against

drugs and the emergence of pneumonia, septicemia, cellulitis, and abscesses (Muthulakshmi and Uma, 2019; Muteeb et al. 2023). A comprehensive analysis of the experimental areas for both types of bacteria revealed more significant inhibition at higher concentrations of nanoparticles for each species. The results showed a dose-dependent effect, where an increase in nanoparticle concentration led to a broader zone. The findings of this study demonstrate that Ag-NP produced from *C. procera* can be effectively utilized as an agent to combat a wide range of illnesses. This highlights the significant potential of these materials for therapeutic applications.

Conclusion

The findings of this study clearly depict that the synthesized silver nanoparticles (Ag-NP) produced using green synthesis techniques from *C. procera* have a potent antibacterial activity. These nanoparticles had a size range of 50-100 nm. Furthermore, the silver nanoparticles exhibited potent antibacterial properties against specific Gram-negative and Gram-positive bacterial strains. Thus, nanotechnology can enhance the efficiency of utilizing traditional plants by coating their biomolecules as a stabilizer on the surface of nanoparticles. As a result, the medicinal properties of the plants could be enhanced at the nano-level. Overall, the Ag-NPs derived by phytofabrication have a broad spectrum of antibacterial action against many strains of pathogenic bacteria.

Author(s), Editor(s) and Publisher's declarations

Conflict of interest
The authors declare no conflict of interest.

Source of funding
None declared.

Contribution of authors
Conceptualization and designing of the study: MM, MSL, SS, RA, RIA. Conduction of experiment and collection of data: MM, MSL, SS. Written first draft of the manuscript: MM, MSL, SS, RA, RIA, MI, IB. Helped to prepare figures and tables: MM, MSL, SS, RA. Statistical analysis of data: MM, MSL, SS, RA, RIA, MI, IB. Revision of the manuscript: MM, MSL, SS, RA, RIA, MI, IB. Final draft read by all authors.

Ethical approval
This study does not involve human/animal subjects, and thus no ethical approval is needed.

Handling of bio-hazardous materials
The authors certify that all experimental materials were handled with care during collection and experimental procedures. After completion of the experiment, all materials were properly discarded to minimize/eliminate any types of bio-contamination(s).

Availability of primary data and materials
As per editorial policy, experimental materials, primary data, or software codes are not submitted to the publisher. These are available with the corresponding author and/or with other author(s) as declared by the corresponding author of this manuscript.

Authors' consent
All authors contributed in designing and writing the entire review article. All contributors have critically read this manuscript and agreed for publishing in IJAaEB.

Disclaimer/editors'/publisher's declaration
All claims/results/prototypes included in this manuscript are exclusively those of the authors and do not inevitably express those of their affiliated organizations/enterprises, or those of the publisher/journal management, and the editors/reviewers. Any product mentioned in this manuscript, or claim rendered by its manufacturer, is not certified by the publisher/Journal management. The journal management disown responsibility for any injury to organisms including humans, animals and plants or property resulting from any ideas/opinions, protocols/methods, guidelines or products included in the publication. The IJAaEB publisher/Management stays impartial/neutral pertaining to institutional affiliations and jurisdictional claims in maps included in the manuscript.

Declaration of generative AI and AI-assisted technologies in the writing process

It is declared that we the authors did not use any AI tools or AI-assisted services in the preparation, analysis, or creation of this manuscript submitted for publication in the International Journal of Applied and Experimental Biology (IJAaEB).

References

Abbas, M., Arshad, M., Rafique, M.K., Altalhi, A.A., Saleh, D.I. et al. (2022). Chitosan-polyvinyl alcohol membranes with improved antibacterial properties contained *Calotropis procera* extract as a robust wound healing agent. *Arabian Journal of Chemistry* 15(5):103766.

Ahmad, S., Munir, S., Zeb, N., Ullah, A., Khan, B. et al. (2019). Green nanotechnology: A review on green synthesis of silver nanoparticles—An ecofriendly approach. *International Journal of Nanomedicine* 14(2019):5087-5107.

Ali, M.H., Azad, M.A.K., Khan, K.A., Rahman, M.O., Chakma, U. et al. (2023). Analysis of crystallographic structures and properties of silver nanoparticles synthesized using PKL extract and nanoscale characterization techniques. *ACS Omega* 8(31):28133-28142.

Aliyu, R.M., Abubakar, M.B., Kasarawa, A.B., Dabai, Y.U., Lawal, N. et al. (2015). Efficacy and phytochemical analysis of latex of *Calotropis procera* against selected dermatophytes. *Journal of Intercultural Ethnopharmacology* 4(4):314.

Antwi, A.N., Owusu, K.B.A., Amoa-Bosompem, M., Williams, N.B., Ayertey, F. et al. (2017). Anti-microbial activities of selected Ghanaian medicinal plants and four structurally similar anti-protozoan compounds against susceptible and multi-drug resistant bacteria. *European Journal of Medicinal Plants* 20(2):1-14.

Asif, M., Yasmin, R., Asif, R., Ambreen, A., Mustafa, M. et al. (2022). Green synthesis of silver nanoparticles (AgNPs), structural characterization, and their antibacterial potential. *Dose-Response* 20(2):15593258221088709.

Conan, P.L., Podglajen, I., Compain, F., Osman, M., Lebeaux, D. et al. (2021). Renal abscess caused by Panton-Valentine leukocidin-producing *Staphylococcus aureus*: report of an unusual case and review of the literature. *Infectious Diseases* 53(2):131-136.

Dawadi, S., Katuwal, S., Gupta, A., Lamichhane, U., Thapa, R. et al. (2021). Current research on silver nanoparticles: synthesis, characterization, and applications. *Journal of Nanomaterials* 2021:1-23.

Deepa, S., Kanimozhi, K., Panneerselvam, A. (2013). Antimicrobial activity of extracellularly synthesized silver nanoparticles from marine derived actinomycetes. *International Journal of Current Microbiology and Applied Sciences* 2(9):223-230.

Falana, M.B., Nurudeen, Q.O. (2020). Evaluation of phytochemical constituents and *in vitro* antimicrobial activities of leaves extracts of *Calotropis procera* against certain human pathogens. *Notulae Scientia Biologicae* 12(2):208-221.

Farahat, E., Galal, T., El-Midany, M., Hassan, L. (2015). Effect of urban habitat heterogeneity on functional traits plasticity of the invasive species *Calotropis procera* (Aiton) WT Aiton. *Rendiconti Lincei* 26:193-201.

Ferdosi, M.F., Khan, I.H., Javaid, A., Nadeem, M., Munir, A. (2021). Biochemical profile of *Calotropis procera* flowers. *Pakistan Journal of Weed Science Research* 27(3):341.

Fijan, S., Kocbek, P., Steyer, A., Vodičar, P.M., Strauss, M. (2022). The antimicrobial effect of various single-strain and multi-strain probiotics, dietary supplements or other beneficial microbes against common clinical wound pathogens. *Microorganisms* 10(12):2518.

Linz, M.S., Mattappallil, A., Finkel, D., Parker, D. (2023). Clinical impact of *Staphylococcus aureus* skin and soft tissue infections. *Antibiotics* 12(3):557.

Lodhi, M.S., Khan, M.T., Aftab, S., Samra, Z.Q., Wang, H. et al. (2021). A novel formulation of theranostic nanomedicine for targeting drug delivery to gastrointestinal tract cancer. *Cancer Nanotechnology* 12:1-27.

Menichetti, A., Mavridi-Printezi, A., Mordini, D., Montalti, M. (2023). Effect of size, shape and surface functionalization on the antibacterial activity of silver nanoparticles. *Journal of Functional Biomaterials* 14(5):244.

Mohamed, N.H., Ismail, M.A., Abdel-Mageed, W.M., Shoreit, A.A.M. (2014). Antimicrobial activity of latex silver nanoparticles using *Calotropis procera*. *Asian Pacific Journal of Tropical Biomedicine* 4(11):876-883.

Murti, Y., Yogi, B., Pathak, D. (2010). Pharmacognostic standardization of leaves of *Calotropis procera* (Ait.) R. Br. (Asclepiadaceae). *International Journal of Ayurveda Research* 1(1):14.

Muteeb, G., Rehman, M.T., Shahwan, M., Aatif, M. (2023). Origin of antibiotics and antibiotic resistance, and their impacts on drug development: a narrative review. *Pharmaceuticals* (Basel). 16(11):1615.

Muthulakshmi, K., Uma, C. (2019). Antimicrobial activity of *Bacillus subtilis* silver nanoparticles. *Frontiers in Bioscience-Elite* 11(1):89–101.

Rabelo, A.C.S., Noratto, G., Borghesi, J., Souza Fonseca, A., Cantanhede Filho, A.J. et al. (2023). *Calotropis procera* (Aiton) Dryand (Apocynaceae): State of the art of its uses and applications. *Current Topics in Medicinal Chemistry* 23(23):2197-2213.

Raghava, S., Mbae, K.M., Umesha, S. (2021). Green synthesis of silver nanoparticles by *Rivina humilis* leaf extract to tackle growth of *Brucella* species and other perilous pathogens. *Saudi Journal of Biological Sciences* 28(1):495-503.

Salomoni, R., Léo, P., Montemor, A.F., Rinaldi, B.G., Rodrigues, M.F.A. (2017). Antibacterial effect of silver nanoparticles in *Pseudomonas aeruginosa*. *Nanotechnology, Science and Applications* 10:115-121.

Sancı, R., Volkan, M. (2009). Surface-enhanced Raman scattering (SERS) studies on silver nanorod substrates. *Sensors and Actuators B*: *Chemical* 139(1):150-155.

Singh, J., Dutta, T., Kim, K.H., Rawat, M., Samddar, P. et al. (2018). Green'synthesis of metals and their oxide nanoparticles: applications for environmental remediation. *Journal of Nanobiotechnology* 16:1-24.

Souza, A.J.M., Lima, C.T., Gonçalves, M.P., da C Souza, P.N., Santana, S.S. et al. (2022). First steps on comprehensive understanding of biosafety and toxicity of natural extract from Calotropis procera seeds, new insights towards sustainability. *Journal of Hazardous Materials Advances* 5:100042.